Minor revisions: **16th February 2012**

Title: **Embankment Dam Probabilistic Assessment for Climate Scenarios**

Primary Author: **Marie-Christine Preziosi** MEng AMIMechE
PhD Student
School of Engineering and Mathematical Sciences
City University London
Northampton Square
London
EC1V 0HB
Office Tel: 020 7040 3308
Mobile: 07703 312 459
e-mail: m.preziosi@city.ac.uk

Secondary Author: **Dr. Tatyana Micic** PhD DIC DipEngCiv
Senior Lecturer in Structural Engineering
School of Engineering and Mathematical Sciences
City University London
Northampton Square
London
EC1V 0HB

ABSTRACT

For small earthfill dams exposed to climate scenarios such as those defined in UKCP09, deterministic assessments are insufficient and more sophisticated models are required. This paper presents a hybrid probabilistic methodology that quantitatively measures the notional reliability index against upstream and downstream slope failure for such dams exposed to variable precipitation. Upstream and downstream slope stability are selected here as representative significant limit states governing the dam's long-term performance. The governing equations for the limit states are defined using the sliding block method incorporating the effects of infiltration through the embankment. Using standard and sloping Green-Ampt and closed form van Genuchten methods, the rainfall effects on soils with variable saturation are considered and the standard First Order Second Moment method applied. The probabilistic model encompasses uncertainties associated with soil properties, dam geometry and rainfall parameters. The paper demonstrates notional reliability indices for the dam for selected precipitation scenarios. A benchmark is developed that reflects the critical conditions conducive to slope failure. The paper reflects on the implication of inclusion of probabilistic climate models on associated risks. Therefore, the analysis is an effective new management tool for risk assessment of embankment dams as categorized by the Flood and Water Management Act 2010.

Keywords: *Embankments; Risk & probability analysis; Public policy*

Notation:

c'	Effective cohesion
CDF	Cumulative Distribution Function
CW	Crest width
e	Void ratio
FM	Failure mode
FORM	Hasofer-Lind transformation method
FOSM	First Order Second Moment Reliability Method
F_p	Cumulative infiltration at t_p
F_x	Cumulative infiltration
G-A	Green Ampt
H	Height of embankment
H_f	Depth of foundation
H_w	Headwater height
i	Infiltration rate
K	Unsaturated hydraulic conductivity
K_r	Relative hydraulic conductivity
K_s	Saturated hydraulic conductivity
LC	London Clay fill
L_x	Depth water has infiltrated
n_s	Porosity
P_a	Total active pressure
$P_{a_{dwn}}$	Total active pressure downstream section before rainfall event
$P_{a_{RIdwn}}$	Total active pressure downstream section during rainfall event
$P_{a_{RIup}}$	Total active pressure upstream section during rainfall event
$P_{a_{up}}$	Total active pressure upstream section before rainfall event
P_f	Probability of failure
P_p	Passive earth pressure
$P_{p_{dwn}}$	Total active pressure downstream section before rainfall event
$P_{p_{RIdwn}}$	Total active pressure downstream section during rainfall event
$P_{p_{RIup}}$	Total active pressure upstream section during rainfall event
$P_{p_{up}}$	Total active pressure upstream section before rainfall event
P_s	Structure's reliability
P_w	Pore water pressure
RI_{fc}	Rainfall Intensity Factor
S_r	Degree of saturation
SWCC	Soil-Water Characteristic Curve
t	Rainfall duration
t_e	Equivalent time to infiltrate a given volume of infiltration
t_p	Time to surface ponding
UKCIP	UK Climate Impacts Programme
UKCP09	UK Climate Projections
X_i	Uncertain random variable
μ	Mean
α_{slp}	Slope angle
γ_d	Dry unit weight of soil
γ_{fc}	Unit weight of soil factor
γ_m	Moist unit weight of soil
γ_{sat}	Saturated unit weight of soil
γ_{sub}	Submerged unit weight of soil
θ_r	Residual moisture content
θ_s	Saturated moisture content
σ	Standard deviation
φ'	Effective internal friction
Φ	Standard normal distribution function
ψ	Wetting front suction head
Θ	Effective saturation of the soil
α_i	Sensitivity factor
β	Reliability index
β_{HL}	Hasofer-Lind reliability index
θ	Moisture Content
$\rho_{\varphi',c'}$	Correlation coefficient for φ' and c' variables
τ	Coulomb's shear strength

1 INTRODUCTION

In this paper we will address issues that are emerging for the built infrastructure in the presence of envisaged climate changes (Gething, 2010). Climate changes will affect embankment dams in general, but very significantly those dams, which are well established and were previously outside the Reservoir Act 1975, but now subject to the new Flood and Water Management Act 2010. Due to insufficient data, decision makers are faced with the problem of obtaining quantitative performance measures for such dams. This paper therefore presents a hybrid probabilistic methodology that quantitatively measures the notional reliability for established small earthfill embankment dams against slope failure when exposed to variable seasonal precipitation. Here, the slope failure represents the significant limit state governing the embankment's long-term performance. As an extension, the methodology will be applicable to other limit states that could develop as well as to other dam types.

In previous years any reservoir with a capacity greater than 25,000 m^3 had to comply with the Reservoir Act 1975, whereas now only those reservoirs whose capacities are below 10,000 m^3 are legally outside the Flood and Water Management Act 2010 (The UK Statute Law Database, 2010). This new legislation also includes new arrangements for reservoir safety based on risk rather than the reservoir's size.

For those earthfill embankment dams, which until now were not covered by the Act, it is unlikely that detailed, consistent, data is available. This could be due to inconsistent monitoring of the dam and/or only a small number of data samples taken over the course of its lifecycle. Therefore, certain properties will either be largely unknown or noticeably differ between the data samples.

By implementing the hybrid probabilistic method, it will be possible to determine how such earthfill embankment dams could be classified according to risk within the Flood and Water Management Act 2010.

In addition, a probabilistic model for future climate projections has been recently established in the form of UKCP09 that will inevitably lead to dam evaluation in terms of climate projections. Such an approach will put emphasis on variability of risk that a sample dam is subject to over diverse time horizons. The envisaged procedure is illustrated in Figure 1, which presents the key stages in the hybrid probabilistic slope stability analysis.

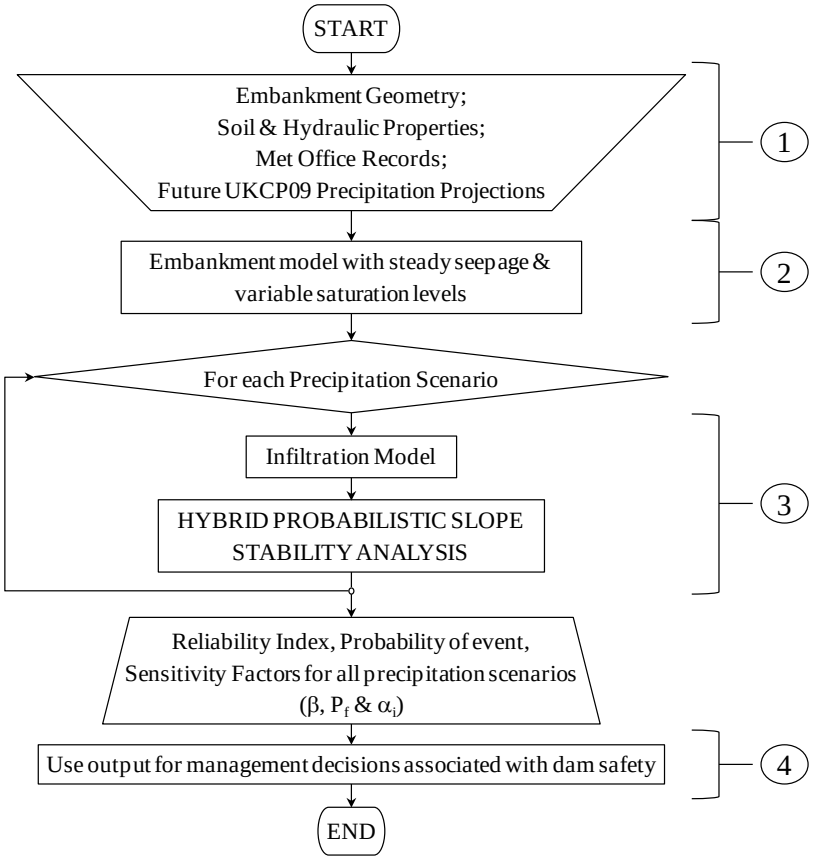

Figure 1. Flowchart for hybrid probabilistic analysis

Recorded failures of earthfill dams can be attributed to seepage, piping, foundation instability, deformation etc. (Johnston et al., 1999), which are all influenced by changes in the surrounding environment due to climate change (Preziosi & Micic, 2009; 2011) and the same probabilistic approach would be applicable. As it will be important to ascertain how environmental factors affect the performance of the infrastructure, for the current analysis, failure due to slope instability (structural failure), seepage failure and environmental factors are selected for consideration, as a representative form of failure. Here only the environmental factor precipitation, in the form of rainfall, is considered as it directly influences the embankment's slope stability. From an experimental study Leong et al. (1999) confirmed that slope failure occurred during or after rainfall and was dependent on the total amount and/or intensity of the rainfall. The probabilistic model will be developed for upstream and downstream slope failure of well established dams where effects, such as the changing climate were not initially considered at the dam's design and construction stage. Uncertainties associated with soil properties, embankment geometry and rainfall parameters, as indicated by step 1 in Figure 1 represent input parameters. Traditional steady seepage model is implemented to establish saturation levels of the fill, step 2 in Figure 1. For the probabilistic analysis of the embankment, the specific infiltration model, step 3 in Figure 1, is defined. As considered embankment dams are assumed to be old and well established, the effect of construction, compaction and settlement of the embankment fill have not been included in the probabilistic analysis. In the same manner an issue could arise about changes to the fill composition over time and due to associated uncertainties probabilistic analysis would be needed to quantify these effects. At present there isn't sufficient data available to account for these effects.

The output of the hybrid probabilistic analysis will represent a tool for decision-makers (Undertakers, Panel Engineers, Environment Agency, etc.), step 4 in Figure 1. The aim is not to replace existing risk assessments, but to improve the quality of data used by the decision-makers. While in this paper a sample limit state is considered, for infrastructure management other limit states would need to be addressed in the probabilistic manner as well so that rational and comprehensive account of uncertainties is made.

2 EMBANKMENT PHYSICAL MODEL

The model is based on a generic long established small homogenous earthfill embankment dam where no drainage was adopted at the downstream toe. It has a known foundation depth (H_f) and an embankment height (H), whose reservoir has reached its maximum allowable capacity (H_w), Figure 2. These forms of embankments are not impervious, causing water to steadily seep through the embankment from the reservoir and/or its foundation over its lifetime. By implementing the standard seepage theory (Cedergren, 1989), the trajectory of the phreatic line through the embankment is expressed as a function of the embankment's slope gradients, geometry and the reservoir's headwater height and used to define the physical model of the embankment. The expression for the position of the phreatic line is thus set out to reflect the site specific uncertainties associated with the dam. As the height of the phreatic line fluctuates, variations in the unit weights of the embankment fill (dry, moist, saturated & submerged) above and below the phreatic line, as illustrated in Figure 2, including the pore water pressures present within the fill are also taken into account.

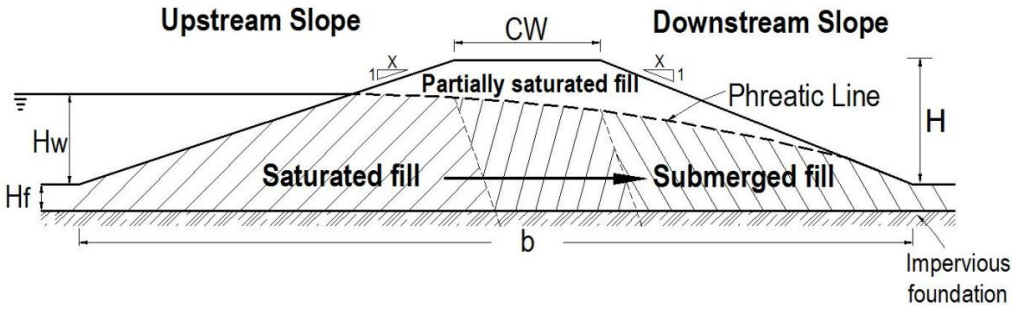

Figure 2. Embankment model

As the dam geometry and the seepage line position are dependant on uncertain variables and therefore uncertain themselves, for application of common limit equilibrium methods (i.e. Method of Slices, Circular Arc Method, etc.) computational meshing would have to reflect the variability in slope domain that needs to be discretized and variability of the soil properties within the domain. Bowles (1984) has pointed out that for Method of Slices errors are associated with the soil properties and the location of the slope's failure, rather than the shape of the assumed failure surface. Both probabilistic modelling and variable hydraulic conductivity within the slope would have been likely to affect the accuracy of this method so it was not implemented. To respond to modelling requirements in the presence of uncertainties and with the view of precipitation scenarios that are due to be implemented, the Sliding Block Method is selected as illustrated in Figure 3 (Tancev, 2005). This incorporates the embankment's geometry, the updated position of the phreatic line, pore pressures acting on the slope and the varying soil conditions as demonstrated by Preziosi & Micic (2009). As outlined by Bowles (1984) and Preziosi & Micic (2009), the vertical and horizontal forces acting on the slope are dependent on its shear strength and resultant active (P_a) and passive (P_p) earth pressures, which are themselves sensitive to the soil's strength parameters and pore water pressures present within the embankment fill. The fill above the phreatic line will have variable saturation levels and corresponding pore water pressures will be included in the formulation. Due to beneficial pore

water pressures within the partially saturated fill zone, effective shear strength parameters for the embankment fill above and below the phreatic line, as illustrated in Figure 3, are incorporated into the Sliding Block Method for the formulation of the forces acting on the slope.

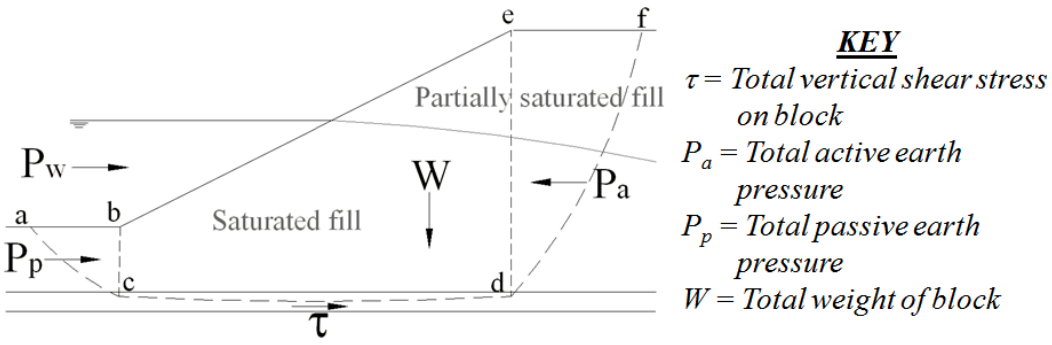

Figure 3. Application of Sliding Block Method for slope stability analysis (Preziosi & Micic, 2011)

By using the Sliding Block Method, a realistic model for the overall stability of the upstream and downstream sections of the embankment when rainfall has traversed through the embankment is established. As explained by el-Ramley et al. (2002), deterministic limit equilibrium methods for slope stability analysis do not consider uncertainties, aleatory and epistemic. Aleatory uncertainty refers to the inherent randomness or natural variations in the physical world (Hartford & Baecher, 2004). This includes geological processes such as the soil properties of the embankment fill (Huber et al., 2011). Epistemic uncertainty relates to the lack of representative data, simplifications and approximations adopted in the geotechnical modelling, etc. (Hartford & Baecher, 2004). This stems from our lack of perfect knowledge due to limited data about the structure, effectiveness of the selected equilibrium method, scale of site tests, etc. (Baecher & Christian, 2003; Faber & Vrouwenvelder, 2008). As the selected analytical model (Sliding Block) is implemented for all analyses, we limit the probabilistic modelling to aleatory uncertainties associated with:

- The embankment geometry.
- The fill's soil properties.
- The reservoir's headwater height.
- Climate effects, specifically diverse precipitation scenarios.

In the current study only soil properties derived from the London Clay type soil have been considered as the embankment's fill, in order to demonstrate the applied methodology. It is a well characterised soil model that could establish a benchmark for future research when effects of the embankment age, fill composition due to any deterioration or strengthening are taken into account. For reference, the probabilistic approach to slope stability problems has been used for 3 clay like soils in Preziosi & Micic (2009), demonstrating that the defined soil model is able to capture the effect of different soil properties. The standard, deterministic, London Clay fill properties, derived unit weights of soil (dry, moist, saturated & submerged), effective internal friction and cohesion of the soil are listed in Table 1.

Table 1. Soil properties & unit weights of soil for London Clay fill (LC)

Soil Properties		**Units**	**LC***
Void ratio (e)			0.79
Moisture content (θ)		%	27 - 29
Cohesion (c')		kN/m^2	7
Internal friction (φ')		°	20
Unit weight of soil	γ_d	kN/m^2	14.9
	γ_m		16.0 – 16.6
	γ_{sat}		19.3
	γ_{sub}		9.5

*Data extracted from (Davis et al., 2008)

3 MODELLING OF PRECIPITATION THROUGH THE EMBANKMENT

Detailed modelling for slope instability due to variable precipitation is now presented, as the fundamental mechanisms of rainfall infiltration through unsaturated soils are still not easily understood (Ng et al., 2003). Variable precipitation is expected to have a noticeable impact on the embankment's reliability.

3.1 Infiltration and Infiltration rate

Infiltration of the water through the embankment fill is considered, as it affects both the properties and behaviour of the soil. The rate water infiltrates through the soil is dependent on the condition of the embankment's surface and vegetation cover, the fill's soil properties such as its porosity, moisture content and hydraulic conductivity (Chow et al., 1988). As stated by Preziosi & Micic (2011), during rainfall the surface layers of the embankment fill become saturated causing the soil's unit weight within these layers to change. Once the water has infiltrated the soil, it advances through the fill saturating further soil layers until the phreatic line is reached, as illustrated in Figure 4. The amount of rainfall absorbed by the soil is dependent on the soil's hydraulic conductivity and corresponding infiltration rate and the time until ponding occurs on the soil's surface.

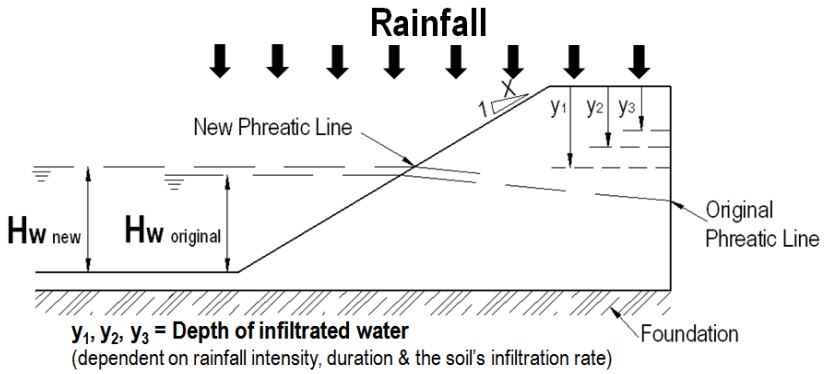

Figure 4. Sketch showing the infiltration of water through the embankment's upstream section

The infiltration rate through the partially saturated slope is initially high, but when the soil layers become more saturated the infiltration rate gradually decreases. This is a direct consequence of changes in soil hydraulic conductivity. To capture the variability in the soil's hydraulic properties for our embankment model in relation to the specific moisture content, we use the van Genuchten method (van Genuchten, 1980). Firstly, we establish the expressions for the unsaturated hydraulic conductivity as a function of the moisture content, also known as soil-water retention curve, (SWCC). The depth water will permeate through the soil depends to a large extent on the soil's hydraulic properties (Wang et al., 2003) and is represented as the wetting front. Due to the high variability of the soil's hydraulic conductivity through the depth of the embankment, representing it as random variable would be too significant a simplification. Thus, we use the soil-water retention curve to characterise the relative hydraulic conductivity at specific depth (function of the moisture content effectively).

3.2 Soil-water retention function (SWCC)

The SWCC can be obtained either experimentally or by using well established empirical methods. However, when taking soil samples from the site, the data obtained may be incomplete due to the great diversity of experimental methods and the quantity of data that needs to be collected. Thus, we apply empirical models to predict the unsaturated hydraulic conductivity from more easily available soil properties, e.g. saturated hydraulic conductivity and fitting parameters (Zhang & van Genuchten, 1994), such as those proposed by Brookes and Corey (1964), Mualem (1976) & van Genuchten (1980) as they produce relatively simple analytical expressions. As a result, the wetting front suction head (ψ) and the unsaturated hydraulic

conductivity (K) of the soil at varying moisture contents (θ) are established using the soil-water characteristic curve, SWCC. The ability to model this process is imperative to perform an accurate assessment of slope stability (Gavin & Xue, 2008).

3.3 van Genuchten method

The van Genuchten method is widely used (Zhou & Yu, 2005) to obtain the relative hydraulic conductivity at a given depth as a function of the saturated hydraulic conductivity (K_s) and the effective saturation of the soil $K(\Theta)$ or corresponding soil water potential $K(\psi)$. The effective saturation of the soil Eqn. (1) and soil water potential are given in Eqns. (2 & 3) respectively, (Jaynes & Taylor, 1984). Hence, the relative hydraulic conductivity (K_r) is given in Eqn. (4).

$$\Theta = \left[\frac{1}{1+(\alpha\psi)^n}\right]^m \quad \text{or} \quad \Theta = \frac{\theta-\theta_r}{\theta_s-\theta_r} \tag{1}$$

$$K(\Theta) = \Theta^{\frac{1}{2}}\left[1-\left(1-\Theta^{1/m}\right)^m\right]^2 \quad \text{(m/s)} \tag{2}$$

$$K(\psi) = \frac{\left\{1-(\alpha\psi)^{n-1}[1+(\alpha\psi)^n]^{-m}\right\}^2}{[1+(\alpha\psi)^n]^{n/2}} \quad \text{(m/s)} \tag{3}$$

$$K_r(\psi) = \frac{K(\psi)}{K_s} \quad \text{or} \quad K_r(\Theta) = \frac{K(\Theta)}{K_s} \quad \text{(m/s)} \tag{4}$$

Where: θ_s = Saturated moisture content; θ_r = Residual moisture content; θ = Measured moisture content; Θ = Effective saturation of the soil; n & α are the empirical fitting parameters of the soil; & m is related to n as m=(1-1/n)

To determine $K(\Theta)$ and $K(\psi)$, the fitting parameters, Table 2, provided by Carsel & Parrish (1988) were implemented. It is these fitting parameters that determine the shape of the SWCC. By applying the soil specific fitting parameters, the value for relative hydraulic conductivity (K_r) at specific depths is determined for partially and/or completely saturated conditions. Even though

the derived soil properties of the London Clay fill are variable, Davis et al. (2008) and Rouainia et al. (2009) applied the same fitting parameters so we have adopted the same parameters in this paper.

Table 2. Soil water retention & hydraulic conductivity parameters for LC

Soil Model	Saturated Hydraulic Conductivity (K_s)**	Fitting parameters (van Genuchten method)***		
	(m/s)	n	m	A
LC	$2.8x10^{-7}$	1.443	0.307	0.458

** Extracted from (Chow et al., 1988); *** Extracted from (Rouainia et al. 2009)

Once the relative hydraulic conductivity K_r and the wetting front suction head ψ are obtained for the soil's saturation level, the specific depth of rainfall infiltration through the embankment needs to be established and, therefore, the slope failure investigated as a function of realistic physical properties. Thus, for depth dependent relative hydraulic conductivity associated with partially saturated soil, the depth that the water has permeated for specific rainfall durations and intensities using actual infiltration rate (i) through the soil will be quantified using the Green-Ampt method.

3.4 Applied Green-Ampt method (G-A)

To establish the depth that the water has permeated vertically through the embankment, subject to rainfall, the Green-Ampt (G-A) method has been applied (Maidment, 1993). This provides an appropriate formulation for determining the depth rainfall has traversed through the embankment fill over the rainfall's duration while still taking into account the hydraulic properties of the soil and the time till ponding (t_p) occurs on the soil's surface. Ponding only occurs once the infiltration rate is greater than the infiltration capacity of the soil (Chow et al., 1988). The G-A

method produces an analytical solution for Richards equation, which is the partial differential equation of infiltration in unsaturated soils for one dimensional vertical flow (Chow et al., 1988). Thus, during and after ponding the surface layers of the soil become saturated causing either overtopping or surface runoff to develop. Since the embankment's crest and slopes are incorporated into the modified slope stability model, the standard G-A method is applied to the crest while the modified G-A method developed by Chen & Young (2006) is applied to both slopes to take into account the slope angle. Hence, when the modified formulation is used the depth of water infiltrated can be expressed in the direction normal to embankment's surface.

The G-A methods must be applied in a consistent manner as illustrated in Table 3. Here, Case 1 refers to circumstances when all rainfall is infiltrated & ponding does not occur; Case 2 refers to situations when ponding can & will occur, where Case 2a defines conditions when all rainfall has infiltrated prior to ponding ($t < t_p$) and Case 2b denotes when ponding occurs & runoff develops ($t \geq t_p$). Table 3 lists the detailed expressions required to calculate the depth of infiltrated water through the flat and sloped surfaces, bearing in mind that the results obtained using the G-A method rely on values for K_r, ψ and θ obtained above.

Table 3. Equations implemented to determine the depth of water infiltrated through a flat and sloped surface, as defined by Maidment (1993) and Chen & Young (2006) respectively

EMBANKMENT SURFACE	CASE 1	CASE 2	
		CASE 2A ($t < t_p$)	CASE 2B ($t \geq t_p$)
FLAT 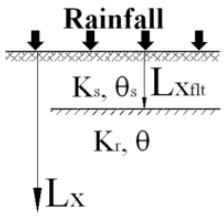	$i_{flt} = i \leq K_r$		$i_{flt} = i > K_r$
	$L_{x_{flt}} = \frac{i_{flt}}{n_s - \theta}$		$F_{P_{flt}} = \frac{\psi(n_s-\theta)}{\left(i_{flt}/K_r\right)-1}$; $t_{P_{flt}} = \frac{F_{P_{flt}}}{i_{flt}}$ $t_{e_{flt}} = \frac{F_{P_{flt}}}{K_r} - \frac{\psi(n_s-\theta)}{K_s} ln\left(1 + \frac{F_{P_{flt}}}{\psi(n_s-\theta)}\right)$
		$L_{x_{flt}} = \frac{i_{flt}}{n_s - \theta}$	$t = t_{P_{flt}} - t_{e_{flt}} + \frac{F_{x_{flt}}}{K_s} - \frac{\psi(n_s-\theta)}{K_s} \ln\left(1 + \frac{F_{x_{flt}}}{\psi(n_s-\theta)}\right)$ $L_{x_{flt}} = \frac{F_{x_{flt}}}{n_s - \theta}$
SLOPED 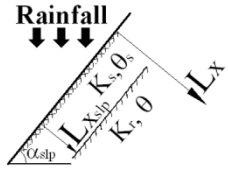	$i_{slp} = i \cos \alpha_{slp}$		$i_{slp} = i \cos \alpha_{slp}$
	$i_{slp} \leq K_r$		$i_{slp} > K_r$
	$L_{x_{slp}} = \frac{i_{slp}}{n_s - \theta}$		$F_{P_{slp}} = \frac{\psi(n_s-\theta)}{\left(\frac{i_{slp}}{K_r}\right)-\cos \alpha_{slp}}$; $t_{P_{slp}} = \frac{F_{P_{slp}}}{i_{slp}}$ $t_{e_{slp}} = \frac{F_{P_{slp}}}{K_r \cos \alpha_{slp}} - \frac{\psi(n_s-\theta)}{K_s \cos \alpha_{slp}} ln\left(1 + \frac{F_{P_{slp}} \cos \alpha_{slp}}{\psi(n_s-\theta)}\right)$
		$L_{x_{slp}} = \frac{i_{slp}}{n_s - \theta}$	$\left[t - \left(t_{p_{slp}} - t_{e_{slp}}\right)\right] K_s \cos \alpha_{slp} = F_{x_{slp}} - \frac{\psi(n_s-\theta)}{\cos \alpha_{slp}} ln\left(1 + \frac{F_{x_{slp}} \cos \alpha_{slp}}{\psi(n_s-\theta)}\right)$ $L_{x_{slp}} = \frac{F_{x_{slp}}}{n_s - \theta}$

Where: i_{flt}, i_{slp} = Infiltration rate for flat and sloped surfaces respectively; t = Rainfall duration; t_{pflt}, t_{pslp} = Time to surface ponding for flat and sloped surfaces respectively; t_{eflt}, t_{eslp} = Equivalent time to infiltrate a given volume of infiltration for flat and sloped surfaces respectively; F_{xflt}, F_{xslp} = Cumulative infiltration for flat and sloped surfaces respectively; F_{pflt}, F_{pslp} = Cumulative infiltration at time of ponding for flat and sloped surfaces respectively; L_{xflt} L_{xslp} = Wetting front depth in the direction normal to the surface; n_s = Porosity; α_{slp} = Slope angle.

3.5 Met Office and UKCP09 data

The UK has a relatively humid climate, thus, precipitation occurs primarily as rain and is recorded by the Meteorological Office, Met Office. The Met Office also keeps detailed climate records dating from 1854 to the present day, including extreme past and historic weather events, and data obtained from weather stations that use the standard instruments and exposure practices.

From these records the Met Office Hadley Centre, for Climate Change Research, developed the climate model HadCM3 simulating future climate change projections (Murphy et al., 2009).

Based on these projections, a detailed assessment of the uncertainties associated with future Climate Projections (UKCP09), for specific variables, was further developed by the UK Climate Impacts Programme (UKCIP). UKCP09 presents these projections as probabilistic ranges (Gething, 2010), which reflect the uncertainties associated with the limitations of the climate model as well as the climate's natural variability (Jenkins et al., 2009). By applying UKCP09, future trends for UK seasonal, annual and monthly temperature, precipitation, etc. can be obtained in probabilistic form (Jenkins et al., 2008). However, UKCP09 cannot be used to estimate probabilistic projections of future changes relating to snowfall rate, latent heat flux, wind speed or soil moisture (Hulme et al., 2002). Yet variations in the soil's moisture content are also dependent on changes in temperature, precipitation, wind speed and solar radiation (Hulme et al., 2002) and will be simulated in simple terms in the following analysis.

As reported in UKCP09, since 1766 the recorded annual mean precipitation over England and Wales has remained relatively consistent. However, (Jenkins et al., 2009) and (Gething, 2010) report that there is a clear shift in seasonal rainfall patterns, including an increase in average rainfall intensity over winter and a change in average seasonal rainfall durations. To determine the future precipitation projections, UKCP09 combines the probabilistic climate change projections with the precipitation recorded during the baseline period (1961-1990). Using the UKCP09 User Interface, these projections are plotted as a Cumulative Distribution Function (CDF) providing the projected distributions for specific climate variables relative to the baseline

climate. The CDFs are available for the projected annual/monthly/seasonal change in precipitation for a given emission scenario, probability level, 30 year time period and location (Jenkins et al., 2009). Sample CDF graphs for seasonal (Winter) and monthly (January) changes in precipitation for high emission scenarios as defined by UKCP09 for the London region are shown in Figure 5.

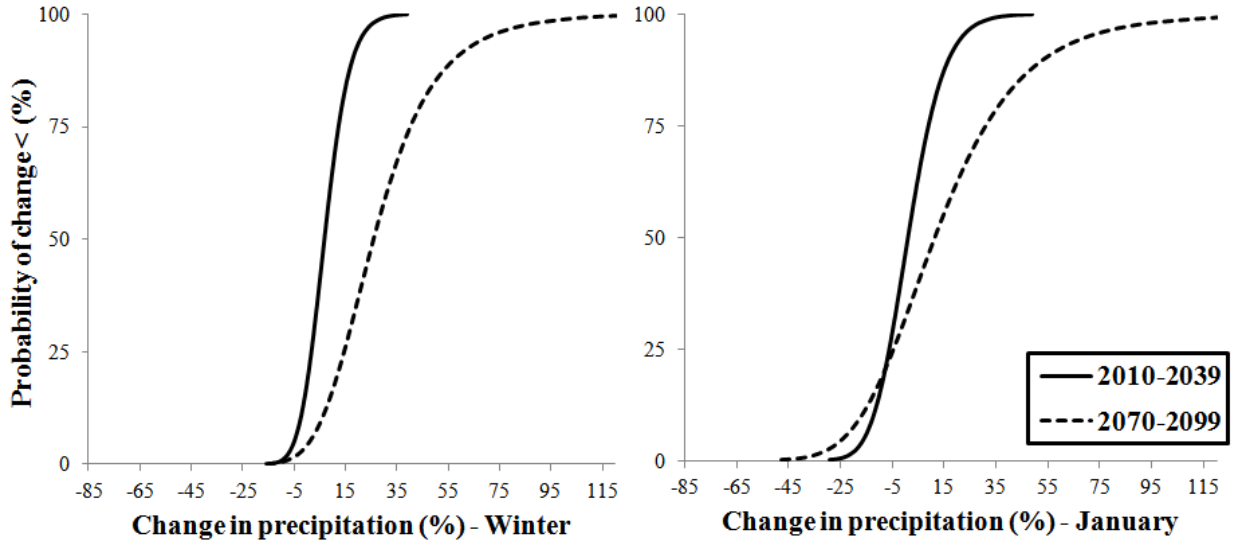

Figure 5. CDF of change in precipitation for high emission scenarios for the Winter and for January: data source UKCP09

It is well understood that the soil's average moisture content will vary noticeably both between the seasons and the regions. Using UKCP09 climate projections and specific past extreme events such as those reported by the Met Office, including short and prolonged rainfalls, different scenarios will be developed to understand their impact on embankment's slope stability.

3.6 Selected Precipitation Patterns

We have considered extensive Met Office data including records of extreme events, such as the Hampstead storm on 14th August 1975 (Met Office, 2010). A selection of past daily, monthly

and extreme precipitation scenarios, labelled A - F, including their average rainfall rates, are presented in Table 4. These rainfall rates were subsequently incorporated into our hybrid probabilistic slope stability analysis to represent relevant events.

Table 4. Past daily, monthly and extreme UK rainfall patterns

Precipitation Scenario	Location & Date	Rainfall Intensity (mm)	Rainfall Duration	Average Rainfall Rate
A[#]	Martinstown 18th July 1955	279.00	24 hrs	11.63 mm/hr
B[##]	England 22nd August 2010	29.25	24 hrs	1.22 mm/hr
C[#]	Maidenhead on 12th July 1901	92.00	60 min	92.00 mm/hr
D[#]	Hampstead 14th August 1975	169.00	2.5 hrs	67.60 mm/hr
E[##]	S England November 1940	185.60	30 days	6.19 mm/day
F[##]	SE England January 1988	158.20	31 days	5.10 mm/day

[#]Extreme events not used for precipitation statistics (Met Office, 2010); [##]Extracted from UK Climate Summaries (Met Office, 2011)

Future precipitation patterns, specifically for the London region, were identified using UKCP09 climate projections for high emission scenarios, such as those in Figure 5. High emission scenarios were selected, as they indicate the 90 % probability level or extreme possible case. As illustrated in Figure 5, the change in precipitation for the winter season and January over selected 30 year periods, 2010-2039 and 2070-2099, would follow diverging trends. Such results are then used to extrapolate extreme future rainfall events for January and July between 2010-2039 and 2070-2099 for the London region. We selected the 95th fractile of the percentage increase in average rainfall for UKCP09 climate projections for high emission scenarios, to provide quantitative measure of change in precipitation. Thus, Table 5 shows the predicted future rainfall intensities for January and July between 2010-2039 and 2070-2099, which were generated and incorporated into the probabilistic model.

Table 5. Probable future rainfall intensities over London incorporating UKCP09 climate projections

UKCP09 Precipitation Scenario	Month & 30 year period	UKCP09 Change in precipitation for High Emission (%)###	Predicted future RI (mm)	Rainfall Duration	Average Rainfall Rate
F1	January 2010-2039	16.98 %	174.13	31days	5.62/ mm/day
F2	January 2070-2099	53.46 %	238.47	31days	7.69 mm/day
C1	July 2010-2039	44.23 %	133.61	1hr	133.61 mm/hr
C2	July 2070-2099	26.81 %	113.33	1hr	113.33 mm/hr

###95^{th} fractile of the percentage increase in average rainfall for UKCP09 climate projections for High Emission Scenarios

Different rainfall patterns and intensities defined in Tables 4 & 5 will be used to establish the variations in the depth of water infiltrated through the dam's embankment fill, see Figure 4. Thus, it will be possible to establish if the embankment's slopes are vulnerable when subject to specific conditions. For the embankment fill above the phreatic line we will consider variable soil saturation levels that would be particularly relevant during the wetter months in winter and at the beginning of spring.

4 APPLICATION OF RELIABILITY ANALYSIS

Firstly, the relevant failure modes (FM) that are assumed to govern the dam's long-term performance are assumed to be failures of the upstream and downstream slopes (FM1 & FM2). Thus, their linear limit state functions prior to and during the rainfall event, Eqns. (5a & 5b) and Eqns. (6a & 6b) respectively, with reference to Figure 3 and Table 3.

$$g(\text{upstream}) = \tau_{up} - \left(P_{a_{up}} - P_w - P_{p_{up}}\right) \quad (5a)$$

$$g(\text{upstream}) = \tau_{RIup} - \left(P_{a_{RIup}} - P_w - P_{p_{RIup}}\right) \quad (5b)$$

$$g(\text{downstream}) = \tau_{dwn} - \left(P_{a_{dwn}} - P_{p_{dwn}}\right) \quad (6a)$$

$$g(\text{downstream}) = \tau_{\text{RIdwn}} - \left(P_{a_{\text{RIdwn}}} - P_{p_{\text{RIdwn}}}\right) \quad (6b)$$

Where: $P_{a_{up/dwn}}$ = Total active pressure acting on the upstream/downstream sections; $P_{p_{up/dwn}}$ = Total passive earth pressure on the upstream/downstream sections; P_w = Pore water pressure from the reservoir acting on the upstream section; $\tau_{up/dwn}$ = Coulomb's shear strength acting on the upstream/downstream sections; $P_{a_{RIup/RIdwn}}$ = Total active pressure acting on the upstream/downstream sections during the rainfall event; $P_{p_{RIup/RIdwn}}$ = Total passive earth pressure on the upstream/downstream sections; $\tau_{RIup/RIdwn}$ = Coulomb's shear strength during rainfall event.

While Eqns. (5a to 6b) appear linear, in reality they are non-linear and include a number of variables that depend on the position of the phreatic line, soil properties and the rainfall intensity. Subsequently, the input variables are identified. Those assumed as deterministic are defined in terms of their characteristic value (e.g. the saturated hydraulic conductivity and saturated moisture content), whereas the variables taken as probabilistic are defined in terms of their mean (μ) and standard deviation (σ) or they have been derived as a function of the random variables, such as the position of the phreatic line. Probabilistic variables are selected to represent the aleatory uncertainties concerned with the embankment's geometry, embankment fill's soil properties and rainfall parameters. For the uncertain variables, we would like to be able to establish a joint probability density function ($f_g(x)$) for $g(X_i)$, where 'g' is a limit state function of the uncertain variables (X_i) and has some distribution function itself. However, that is not feasible in most cases. Therefore, for the limit state functions as defined in Eqns. (5 & 6) a generic notation X_i was introduced and the probability of failure (P_f) for FM1 and FM2 evaluated, Eqn. (7). As a complement to P_f, the structure's reliability (P_s) can also be obtained, Eqn. (8), and a commonly used reliability index, Eqn. (9).

$$P_f = P[g(X_i) \leq 0] = \int_{g(x)\leq 0} f_g(x)dx = \Phi(-\beta) \quad (7)$$

where Φ is the standard normal distribution function

$$P_s = 1 - P_f \quad (8)$$

From Eqn. (7) it can be shown that β is related to the probability of failure by:

$$\beta = -\Phi^{-1}(P_f) \quad (9)$$

Equation 7 is deceptively simple, as the integral includes uncertainties associated with the joint density function, $f_g(x)$, and with the failure domain (when $g(X) \leq 0$). From Eqn. (9) it can be observed that the higher reliability index reflects low probability of failure. For the evaluation of the integral in Eqn. (7) the Advanced First Order Second Moment Reliability Method that was developed by Hasofer & Lind (1974) is implemented. The methodology includes the Hasofer-Lind transformation method (FORM/SORM) that could be applied to linear and nonlinear limit state functions, (Haldar & Mahadevan, 2000). Standard Rackwitz-Fiessler iterative approach (Haldar & Mahadevan, 2000) is implemented to determine the most probable failure point within the domain, thus the one with the lowest reliability index.

The reliability methodology is here integrated with the modified deterministic slope stability model to create the hybrid probabilistic slope stability model. This methodology can be applied when the limit state functions, such as Eqns. (5 & 6), have correlated or non-correlated random variables. The results obtained for each failure mode include the reliability index (β), failure probability (P_f) and sensitivity factors (α_i) that reflect the importance of uncertain variables (Haldar & Mahadevan, 2000). Thus, the sensitivity indices reflect the contribution of the inherent variability of the random variable on the reliability in respect to each limit state.

Finally, the overall safety of the dam, in relation to its slopes, can be expressed in terms of engineering risk. Risk is commonly defined as the product of the probability of the event and the consequence of the event (Hartford & Baecher, 2004), Eqn. (11).

$$\text{Risk} \equiv P_f \times \text{consequence} \tag{11}$$

Here the term 'consequence' will inevitably relate to the consequences caused by the dam failure. These are associated with impacts in the downstream section, including any areas surrounding the dam or appurtenances (Hartford & Baecher, 2004). Currently dam failures are said to be low probability, high-consequence events. However, by analysing the notional reliability and probability of failure of the dam slopes, subject to precipitation, the overall risk arising from climate projections can be assessed for specific failure events, by using Eqn. (11) and therefore, the true risk exposure quantified.

5 PROBABILISTIC SLOPE STABILITY ASSESSMENT OF EMBANKMENT DAM

Probabilistic slope analysis is carried out for failure modes defined in Eqns. (5a to 6b)

5.1 Probabilistic modelling of uncertain variables

It is difficult to accurately measure the embankment's geometry, especially if the dam is still operational. So, indirectly, the embankment's physical model has to be treated as uncertain. Here the mean values and standard deviation of the embankment's height, crest width and foundation are modelled using normal distribution, Table 6. As an extension, by probabilistically modelling the geometry the position of the trajectory of the phreatic line would reflect variations in the upstream and downstream slope gradients caused by localised changes such as dipping or crest

reduction due to soil degradation at the embankment's surface, external erosion of the slopes, bulging at the downstream toe and improvements to the slopes during maintenance or repair.

When modelling the phreatic line, it was assumed that the dam's headwater height was maintained at its maximum allowable level over a significant period time. However, the reservoir level is subject to change due to environmental effects, such as rainfall or evaporation, or due to inaccuracies in measurements of the reservoir's water level by the Inspecting Engineer. For that reason, the headwater height is presumed to be uncertain and modelled as probabilistic with normal distribution, as in Table 6. Larger, visible, changes are more commonly associated with rapid drawdown of the reservoir or overtopping due to flooding so would initiate a separate failure mode and are not taken into account here.

For the soil properties relating to the London Clay fill, it is difficult to obtain reliable experimental data samples, so probabilistic modelling of the soil parameters was developed from reported sample soils assuming homogenous embankment dam. Derived unit weights of soil (dry, moist, saturated & submerged), above and below the phreatic line are directly affected by:

- The soil's moisture content or degree of saturation.
- The relative hydraulic conductivity and suction head of the soil.

Therefore, for modelling the unit weight of soil within the upstream, core and downstream sections of the embankment, a unit weight of soil factor (γ_{fc}) is introduced to account for variations between soil samples. It is assumed that the unit weight of soil is normally distributed and its mean value and standard deviation are presented in Table 6.

As defined in the JCSS Probabilistic Model Code (Baker & Calle, 2006) and by Liang et al. (1999), for any geotechnical reliability analysis, the uncertainties resulting from the unit weight, internal friction and cohesion of the soil are assumed to have normal (Gaussian) probability distribution. Pumjan & Young (1999) observed that when modelling the geotechnical strength parameters (cohesion, internal friction and density variables), cohesion and internal friction were found to be interdependent and negatively correlated. Cherubini (2000) also noted that when performing a probabilistic analysis on shallow foundations, when cohesion and internal friction were negatively correlated ($\rho_{\varphi',c'}$ = 0 to -0.75) the evaluated reliability index was higher than that obtained when the variables were uncorrelated. Therefore, the soil's internal friction (φ') and cohesion (c') are said to be normally distributed and assumed to be negatively correlated (-0.5), see Table 6.

It is evident that probabilistic modelling is site specific, so if this approach is applied to many sites, specific guidelines from the regulatory body would be required to address the sources of information and appropriate modelling techniques that should be used.

Table 6. Probabilistic modelling of the input parameters: Variables are normally distributed

Variable	Unit	Mean (μ)	Standard deviation (σ)
Height (H)	m	3.0	0.150
Crest Width (CW)	m	2.8	0.028
Height of foundation (H_f)	m	0.5	1.000
Headwater height (H_w)	m	2.0	0.100
Internal friction (φ') ✦	°	20.0	2.000
Cohesion (c') ✦	kN/m^2	5.0	0.500
Unit weight of soil factor (γ_{fc})	kN/m^2	1.0	0.100
Rainfall Intensity factor (RI_{fc})	mm	1.0	0.100

✦Negatively correlated (-0.5)

5.2 Probabilistic analysis for selected precipitation scenarios:

Over its lifetime, the dam is continually exposed to changes in its surrounding environment. This will result in a variable degree of saturation, relative hydraulic conductivity and unit weight of soil above the phreatic line. As an example, when the moisture content (θ_r) of the London Clay fill's surface layers increases from 56 % to 76 %, its relative hydraulic conductivity will vary from $4.9x10^{-8}$ to $5.7x10^{-7}$ m/s, while the wetting front suction head (ψ) decreases from approximately 7.3 to 2.8 cm. To account for the high variability in relative hydraulic conductivity the coupled Van Genuchten-Green Ampt approach described earlier has been implemented to model the variation over the depth. For instance, during the winter months the fill's saturation level will be high resulting in a higher unit weight of soil, compared to those recorded over the summer months. Therefore, the shear stress of the slopes will increase while simultaneously decreasing their shear strength. This will result in the reliability indices, β_{up} & β_{dwn}, for upstream (FM1) and downstream (FM2) slope failure to differ. For the current parametric study, since the soil's degree of saturation (S_r) vary between seasons, two extreme soil saturation levels were considered, S_r = 57 % & 86 %. Thus, for each precipitation scenario and degree of saturation, the reliability index and associated depth of water infiltrated for each failure mode as defined in Eqns. (5a to 6b) were obtained.

5.3 Deterministic results: Depth of water infiltrated for precipitation scenarios

For both limit states and saturation cases, the depth to which the water has infiltrated through the slopes, L_{up} & L_{dwn}, was obtained for different rainfall durations and intensities, and are shown in Table 7. When S_r = 57 % the amount of rainfall infiltrated through the embankment is relatively small. Meaning the residual rainfall retained on the embankment's surface could instigate slope

failure in the form of runoff or overtopping. In the case of precipitation scenarios A – D, C1 & C2, high rainfall intensity over a short duration, only the surface layers of the embankment are completely saturated as the depth of water infiltrated is small. However, the rainfall duration clearly influences the depth of water infiltrated, as shown by results for precipitation scenarios E, F, F1 & F2 in Table 7. This demonstrates the effect of prolonged rainfall, on the depth of water infiltrated as a function of the fill saturation, rainfall intensity and duration.

Table 7. Depth of water infiltration through the slope, including time taken to reach the phreatic line for the precipitation scenarios with varying S_r

Precipitation Scenarios[++]		Depth of water infiltration through embankment slopes (cm) or time to complete failure			
		S_r = 57%		S_r = 86 %	
		L_{up}	L_{dwn}	L_{up}	L_{dwn}
No Rainfall		-	-	-	-
Past precipitation Scenarios	A	3.42	3.42	49.40	50.31
	B	3.39	3.40	47.72	48.68
	C	0.66	0.66	3.89	3.92
	D	1.05	1.05	7.49	7.58
	E	24.98	25.17	9 days[+]	9 days[+]
	F	25.45	25.65	11 days[+]	11 days[+]
UKCP09 precipitation Scenarios	F1	25.50	25.70	10 days[+]	10 days[+]
	F2	25.60	25.79	8 days[+]	7 days[+]
	C1	0.66	0.66	3.89	3.93
	C2	0.66	0.66	3.89	3.93

[+]Approximate time required for infiltrated water to reach the phreatic line; [++] Defined in Table 4 & 5.

By recording the depth water has infiltrated through the embankment fill for each scenario it will be possible to obtain quantitative information about the dam's performance as well as time to failure, as for scenarios E & F. While extreme saturation scenarios are considered here, in practice it is possible to consider genuine site specific conditions.

5.4 Reliability index (β) for FM1 & FM2

From the reliability analyses, the reliability indices, β_{up} and β_{dwn}, for the two failure modes were obtained and are shown in Table 8. The results presented show that variable rainfall intensity and duration greatly affect the slope's overall reliability. By comparing β_{up} and β_{dwn} with the depth rainfall has infiltrated through the embankment slopes, there is a clear correlation between their reliability index and the precipitation scenario. This is evident when the embankment is deemed saturated, S_r = 86 %. As expected, prolonged rainfall over a month (precipitation scenario E, F, F1 & F2) will cause both the upstream and downstream slopes to eventually fail, however the indication is that time to perceived failure is shorter then that obtained from deterministic analysis.

Table 8. Reliability index for FM1 & FM2 for the different precipitation scenarios with varying S_r

Precipitation Scenario[++]		Reliability Index (β)			
		S_r = 57%		S_r = 86 %	
		β_U	β_D	β_U	β_D
No Rainfall		3.19	2.79	3.15	2.79
Past precipitation Scenario	A	2.93	2.47	F[†] (18 hrs)	1.02
	B	2.92	2.47	F[†] (19 hrs)	1.07
	C	3.08	2.57	2.83	2.52
	D	3.06	2.56	2.63	2.40
	E	1.70	1.73	F[†] (6 days)	F[†] (8 days)
	F	1.68	1.71	F[†] (7 days)	F[†] (10 days)
UKCP09 precipitation Scenario	F1	1.68	1.71	F[†] (6 days)	F[†] (9 days)
	F2	1.67	1.71	F[†] (5 days)	F[†] (7 days)
	C1	3.08	2.57	2.83	2.52
	C2	3.08	2.57	2.83	2.52

[++] Defined in Table 4 & 5; [†] Indicates slope failure has occurred as $\beta \leq 1.0$ (F = Slope Failure)

From Table 8, short rainfall scenarios C1 and C2 will not significantly affect the reliability index of the individual slopes irrespective of the moisture content. Yet, for scenarios A and B (24 hrs) both slopes are close to failure even with low rainfall intensities when the fill is highly saturated.

As expected, for the considered embankment model, slope failure is more likely to occur during prolonged rainfall. However, when we compare outcomes shown in Tables 7 & 8, the probabilistic approach provides further information that reveals that slope failure will be deemed to occur prior to the embankment fill above the phreatic line becoming completely saturated. In effect, the information from probabilistic analysis could be used for emergency action planning as information can be provided for a number of days that it will take for dam to reach what is agreed to be failure state. Obtained reliability indices have associated probability of failure as in Eqn. (7) and thus would inform us on the risk level associated with individual limit states, Eqn. (11).

5.5 Sensitivity factors

From the completed analyses, if we consider precipitation scenario C, the variables which have the greatest impact on the limit state's reliability are associated with the fill's soil properties, namely, cohesion, internal friction and the unit weights of the soil. In general this information about sensitivity factors can be used to identify variables, which should be investigated further to update the probabilistic model reducing the uncertainty and, consequently increase the reliability as shown by Preziosi & Micic (2011). The sensitivity factor for rainfall intensity will be variable to a high level between different limit states, e.g. slope stability, overtopping or runoff.

6 IMPLEMENTATION OF RESULTS WITH FLOOD AND WATER MANAGEMENT ACT 2010

The results obtained from the hybrid probabilistic slope stability model can be used as means of determining whether the considered embankment dam should be categorised as either ‘High’ or ‘Low’ risk under the new Act. This could be achieved by looking at the impact dam failure would have on the loss of life downstream of the embankment. As a result, low risk reservoirs would be subject to less stringent regulations, compared to those deemed high risk. In reality if a dam such as the one modelled here is classified as low risk and there is prolonged rainfall, such as those associated with climate projections, the risk classification would need to change as significant damage could threaten the area downstream of the embankment, due to complete slope failure. Yet, for a short rainfall with high rainfall intensity, overtopping or runoff would occur and could lead to flooding downstream, as the embankment fill cannot absorb the excess rainfall. Thus such alternative limit states would become a base for risk classification as they have associated probability of occurrence, Eqn. (11).

It is right that the Flood and Water Management Act 2010 is considering risk as a relevant measure. However, current classifications are not sufficiently detailed as specific dams will have fairly constant consequences, but failure events are not associated with equal probability of occurrence. Therefore, it is important to carry out relevant probabilistic analyses to establish true levels of risk according to the new regulation.

7 SUMMARY OF FINDINGS

This paper has considered the issues that arise due to the implementation of the Flood and Water Management Act 2010 and the latest climate projections in the form of UKCP09 in respect to a generic small earthfill embankment. As the effect of the new probabilistic precipitation models have been identified, comprehensive modelling for the water infiltration through the embankment and a hybrid probabilistic analysis for selected failure modes have been set out. In addition to precipitation scenarios defined in UKCP09, past records of extreme rainfall were also considered in order to develop future extreme event scenarios.

- Probabilistic analyses presented for upstream and downstream slope stability provide useful information about the behaviour of slopes in the presence of site specific uncertain factors and different precipitation scenarios.
- Notional reliability indices for the sample dam and selected precipitation scenarios were shown to provide a quantitative measure of the likelihood of slope failure and can provide improved risk estimates for the dam.
- By applying the UKCP09 climate projections, it is now possible to investigate the quantitative effect of alternative future precipitation scenarios for selected time horizons and, in particular, associated risk. This information can be used for emergency planning and selection of remedial actions.
- The probabilistic approach should be extended to other limit states which could have a significant effect on the embankment dam so that the uncertainty is quantified in a consistent manner. Associated risks should be used for infrastructure management rather then current relatively simple measure.

- Probabilistic analysis provides useful quantitative measures of effectiveness of any remedial measures through updating of probabilistic modelling for relevant variables.
- Application of the probabilistic methodology enables better evaluation of the risk due to the dam's current status and any future conditions. In that respect, it is recommended that risk qualification within the regulatory documentation should be reviewed.
- It would be of benefit if this hybrid probabilistic approach is applied to the network level, i.e. for assessment of all dams, in which case the application of the probabilistic approach would need to be strictly defined in the regulatory documentation.

The work presented here is the first attempt to incorporate future climate projections into standard engineering analysis. Further development with respect to the probabilistic approach is required to establish the modelling for alternative limit states, correlation between limit states and inclusion of site specific information. A more comprehensive soil mechanics model could be developed if it becomes feasible to obtain relevant experimental data to establish probabilistic models for mechanical properties at variable saturation levels. With intense advances in sensing technology experimental data is increasingly improving so much that improved probabilistic modelling can be envisaged. In addition, this hybrid probabilistic methodology can be expanded to consider alternative dam profiles, embankment fills and varying rainfall rates. Thus, enabling a more detailed evaluation of the level of risk due to the current status of the dam and any future conditions at the dam site.

8 REFERENCES

Baecher, G. B. & Christian, J. T. (2003) *Reliability and Statistics in Geotechnical Engineering*. Chichester, John Wiley

Baker, J. & Calle, E. (2006) *Probabilistic Model Code, Section 3.7: Soil Properties, Updated Version. Technical report*, Joint Committee on Structural Safety (JCSS)

Bowles, J. E. (1984) *Physical and Geotechnical Properties of Soils*. 2nd edition. New York; London, McGraw-Hill

Brooks, R. H. & Corey, A. T. (1964) Hydraulic properties of porous media. *Hydrol. Pap* **3**. Colo.State Univ., F. Collins

Carsel, R. F. & Parrish, R. S. (1988) Developing joint probability distributions of soil water retention characteristics, *Water Resources Research* **24**, No. 5, 755-769.

Cedergren, H. R. (1989) *Seepage, Drainage, and Flow Nets*. New York, Wiley (eds.)

Chen, L. & M. H. Young (2006) Green-Ampt infiltration model for sloping surfaces. Water Resour. Res. 42, No. 7: W07420

Cherubini, C. (2000) Reliability evaluation of shallow foundation bearing capacity on c′, φ′ soils. Canadian Geotechnical Journal 37, 264-269

Chow, V. T., Maidment, D. R. & Mays, L. W. (1988) *Applied Hydrology*. McGraw-Hill

Davis, O., Rouainia, M., Glendinning, S. & Birkenshaw, S. (2008) *Assessing the Influence of Climate Change on the Progressive Failure of a Railway Embankment. In: Geomechanics in the Emerging Social & Technological Age* (CD Proceedings, 12th IACMAG Conference, Goa, India, October 2008). Paper No. Q06. Toronto: X-CD Technologies Inc

El-Ramley, H., Morgenstein, N.R. & Cruden, D.M. (2002) Probabilistic slope stability analysis for practice. *Canadian Geotechnical Journal* **39**, 849-862

Faber, M. H. & Vrouwenvelder, A. C. W. M. (2008) Background Documents on Risk Assessment in Engineering, *Background Document #2: Interpretation of Uncertainties and Probabilities in Civil Engineering Decision Analysis.* Joint Committee on Structural Safety (JCSS)

Gavin, K. & Xue, J. F. (2008) A simple method to analyze infiltration into unsaturated soil slopes. *Computers and Geotechnics* **35**, No. 2, 223-230

Gething, B. (2010). *Design for Future Climate: Opportunities for adaptation in the built environment*. Technology Strategy Board

Haldar, A. & Mahadevan, S. (2000) *Probability, Reliability and Statistical methods in Engineering Design*. NY, John Wiley & Sons

Hartford, D. N. D. & Baecher, G. B. (2004) *Risk and uncertainty in dam safety*. London, Thomas Telford Publishing

Hasofer, A. M. & Lind, N.C. (1974) Exact and Invariant Second-Moment Code Format. *Journal of the Engineering Mechanics Division, ASCE*, Vol. 100, 111-121.

Huber, M., Vermeer, P. A. & Moormann, C. (2011) Evaluation and implications of soil variability in tunnelling. *Proceedings of the 11th International Conference on Applications of Statistics and Probability in Civil Engineering (ICASP 2011)*, Zürich, Switzerland, 2785-2791

Hulme, M., Turnpenny, J. & Jenkins, G. (2002) *Climate Change Scenarios for the United Kingdom: The UKCIP02 Briefing Report*. Tyndall Centre for Climate Change Research, School of Environmental Sciences, University of East Anglia, Norwich, UK.

Jaynes, D. B. & Taylor, E. J. (1984) Using Soil Physical Properties to Estimate Hydraulic Conductivity. *Soil Science* **138**, 298–305

Jenkins, G. J., Murphy, J. M., Sexton, D. M. H., Lowe, J. A., Jones, P. & Kilsby, C. G. (2009) *UK Climate Projections: Briefing report*. Met Office Hadley Centre, Exeter, UK

Jenkins, G. J., Perry, M. C. & Prior, M. J. (2008) *The climate of the United Kingdom and recent trends*. Met Office Hadley Centre, Exeter, UK

Johnston, T. A., Millmore, J. P., Charles, J. A., & Tedd, P. (1999) *An engineering guide to the safety of embankment dams in the United Kingdom*. 2nd edition. BRE Report: BR 363

Leong, E. C., Low, B. K., & Rahardjo, H. (1999) Suction profiles and stability of residual soil slopes. *Slope Stability Engineering*, Vol. 1, 387-390

Liang, R. Y., Nusier, O. K. & Malkawi, A. H. (1999) Reliability Based Approach For Evaluating The Slope Stability Of Embankment Dams. *Engineering Geology* **54**, 271-285

Maidment, D. R. (1993) *Handbook of hydrology*. McGraw Hill

Met Office. (2011) Available at: http://www.metoffice.gov.uk/climate/uk/

Met Office. (2010) Available at: http://www.metoffice.gov.uk/climate/uk/extremes/

Mualen, Y. (1976) A new model of predicting the hydraulic conductivity of unsaturated porous media, *Water Resour. Res*. ***12***, 513–522

Murphy, J. M., Sexton, D. M. H., Jenkins, G. J., Boorman, P.M., Booth, B. B. B., Brown, C.C., Clark, R. T., Collins, M., Harris, G. R., Kendon, E. J., Betts, R.A., Brown, S. J., Howard, T. P., Humphrey, K. A., McCarthy, M. P., McDonald, R. E., Stephens, A., Wallace, C., Warren, R., Wilby, R. & Wood, R. A. (2009) *UK Climate Projections Science Report: Climate change projections*. Met Office Hadley Centre, Exeter

Ng, C.W.W., Zhan, L. T., Bao, C. G., Fredlund, D. G. & Gong, B.W. (2003) Performance of an Unsaturated Expansive Soil Slope Subjected to Artificial Rainfall Infiltration. *Géotechnique* **53**, No. 2, 143–157

Preziosi, M-C. & Micic, T. (2009) Probabilistic assessment of small earthfill dams subject to adverse climate effects. *Proc. ICOSSAR 2009*, Osaka, Japan

Preziosi, M-C. & Micic, T. (2011) Probabilistic assessment of small earthfill dams subject to variable precipitation. *Proc. ICASP11*, Zurich, Switzerland

Pumjan, S. & Young, D. S. (1999) Geotechnical site characterisation in localized probabilistic terms. *Proc. 37th US Symp. Rock. Mech (USRMS)*. Vol. 2, 801-808

Rouainia, M., Davies, O., O'Brien, T. & Glendinning, S. (2009) Numerical modelling of climate effects on slope stability. *Proceedings of the Institution of Civil Engineers - Engineering Sustainability* **162**, No. 2, 81-89

Tancev, L. (2005) *Dams and appurtenant hydraulic structures*. Leiden; London: Taylor & Francis

The UK Statute Law Database (2010) *Flood and Water Management Act 2010* (c.29)

van Genuchten, M. T. (1980) A closed-form equation for predicting the hydraulic conductivity of unsaturated soils, *Soil Science Society of America Journal* **44**, 892– 898

Wang, Q., Shao, M. & Horton, R. (2003) A simple method for estimating water diffusivity of unsaturated soils. *Soil Science Society of America Journal* **68**, 713–718

Zhang, R. & van Genuchten, M. T. (1994) New Models for Unsaturated Soil Hydraulic Properties. *Soil Science* **158**, No. 2, 77-85

Zhou, J. & Yu, J-l. (2005) Influences affecting the soil-water characteristic curve. *Journal of Zhejiang University SCIENCE* **6A**, No. 8, 797-804